Supplementary Fig. 1.

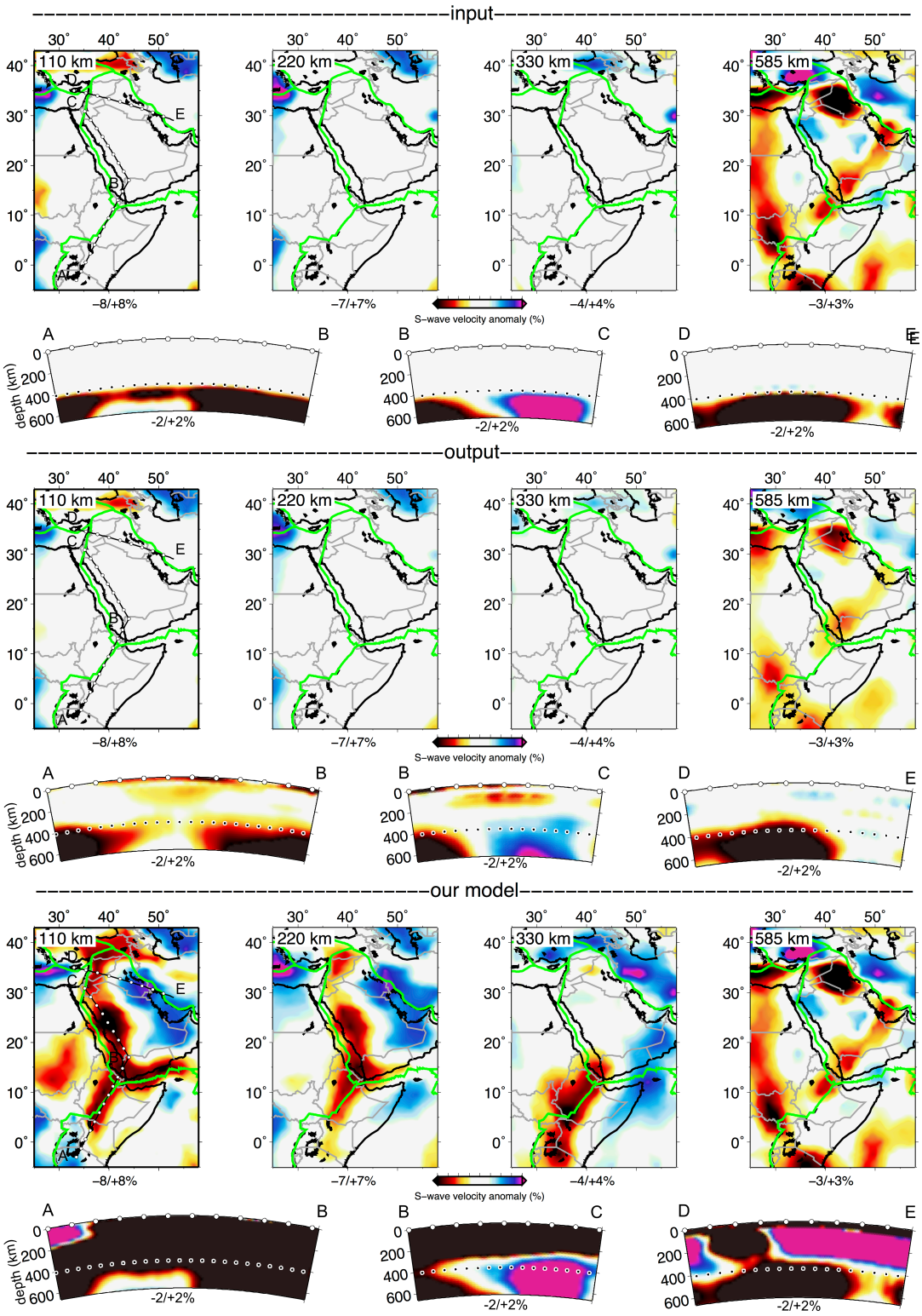

Structural resolution test. The velocity anomalies are removed in the input (top panels) at depths shallower than 410 km depth. The output model (middle panels) shows that most of the structure removed does not appear in the upper mantle above 410 km depth. The magnitude of the spurious structure below East Africa-Arabia is weaker than that imaged in our model (bottom panels). The orientations of the cross-sections are plotted in the 110-km depth slice. Major plate boundaries are plotted as green lines. White points indicate the distance every 2°. The dotted line in the cross-sections indicates the 410-km depth discontinuity.

Supplementary Fig. 2.

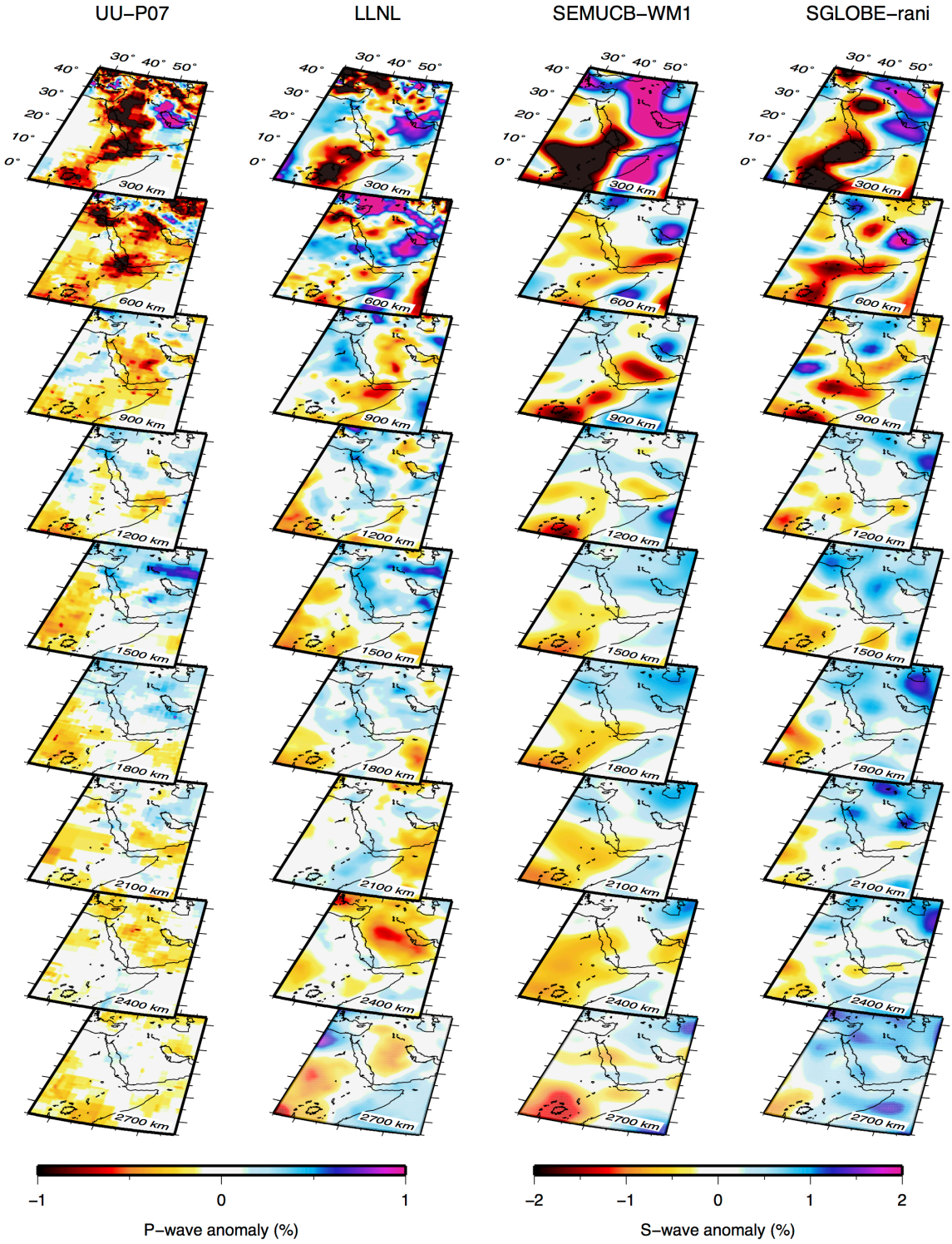

Global tomographic models through the whole mantle. Tomographic depth slices are shown for the following whole-mantle tomography models: the P-wave model UU-P07 (Amaru, 2007) in the first column; the P-wave model LLNL (Simmons et al., 2012) in the second column; the S-

wave model SEMUCB-WM1 (French & Romanowicz, 2014) in the third column; and the S-wave model SGLOBE-rani (Chang et al., 2015) in the fourth column.

Supplementary Fig. 3.

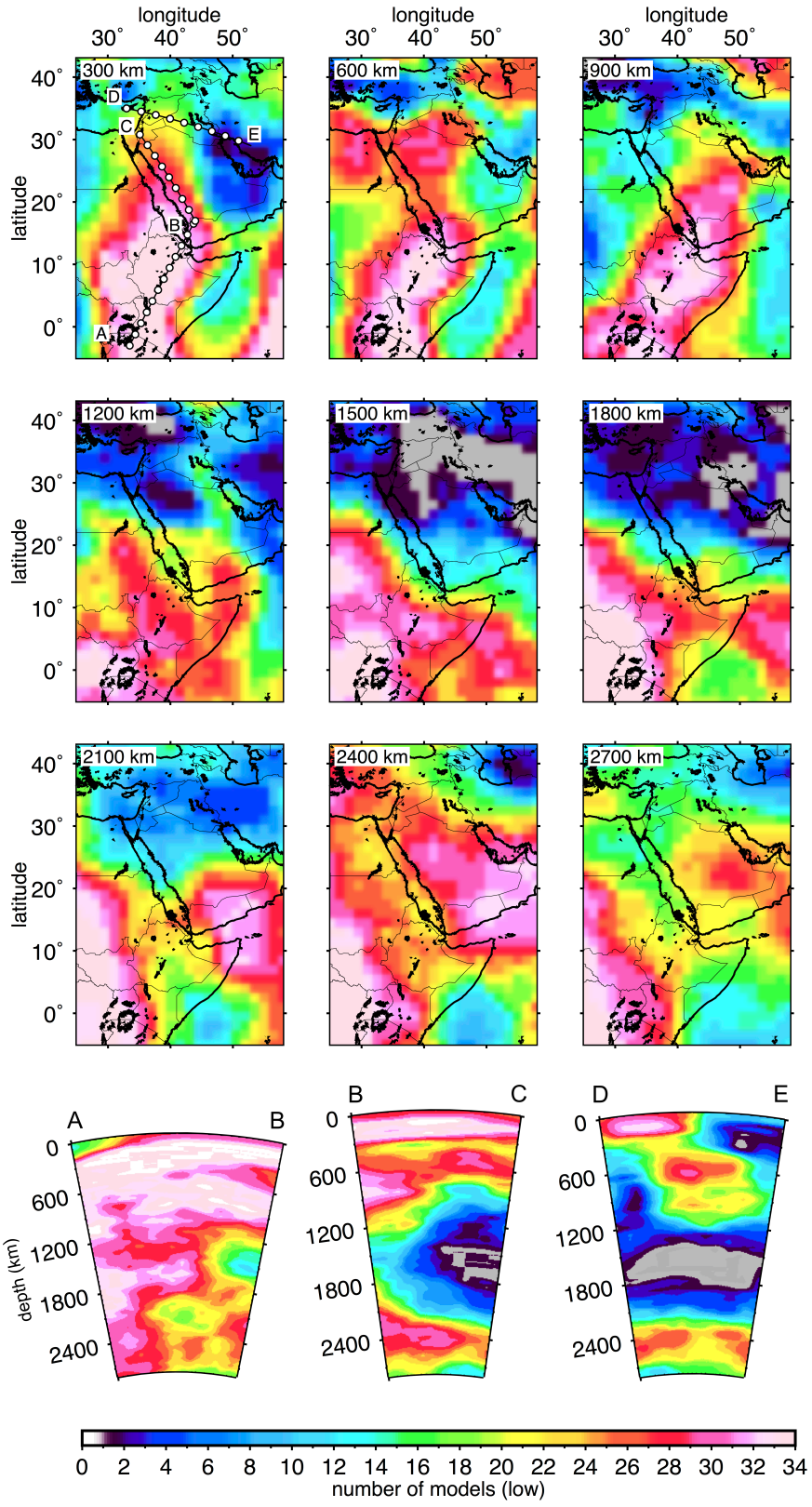

Low-velocity vote images of the whole mantle for 34 tomographic models (dv/v < 0). The vote maps and cross-sections are obtained by the joint analysis of *P*- and *S*-wave models available in the *SubMachine* tomography repository (Hosseini et al., 2018). The number of votes at a given location corresponds to the number of models in which a seismically slow velocity anomaly at a given depth is present. The models are those used in Supplementary Figure S8. The vote maps highlight a broad low-velocity anomaly below southern Arabia and offshore Somalia at 2100-2400 km depth, which may indicate the deep mantle roots of the LP and AP. Another low-velocity body below Central-East Africa underlies the KP and is likely to be its deep part. The orientations of the cross-sections are plotted in the depth slices at 300 km. Cross-section AB shows an overwhelming model agreement on the presence of a low-velocity anomaly below East Africa down to the base of the lower mantle. The maximum vote region is below Kenya and Tanzania. In cross-section BC high vote counts are observed mostly in the asthenosphere beneath West Arabia, in agreement with the low-velocity channel imaged in our model. Cross-section DE captures the shape and extension of the low-velocity anomaly imaged below the Levant region, interpreted as the LP.

Supplementary Fig. 4.

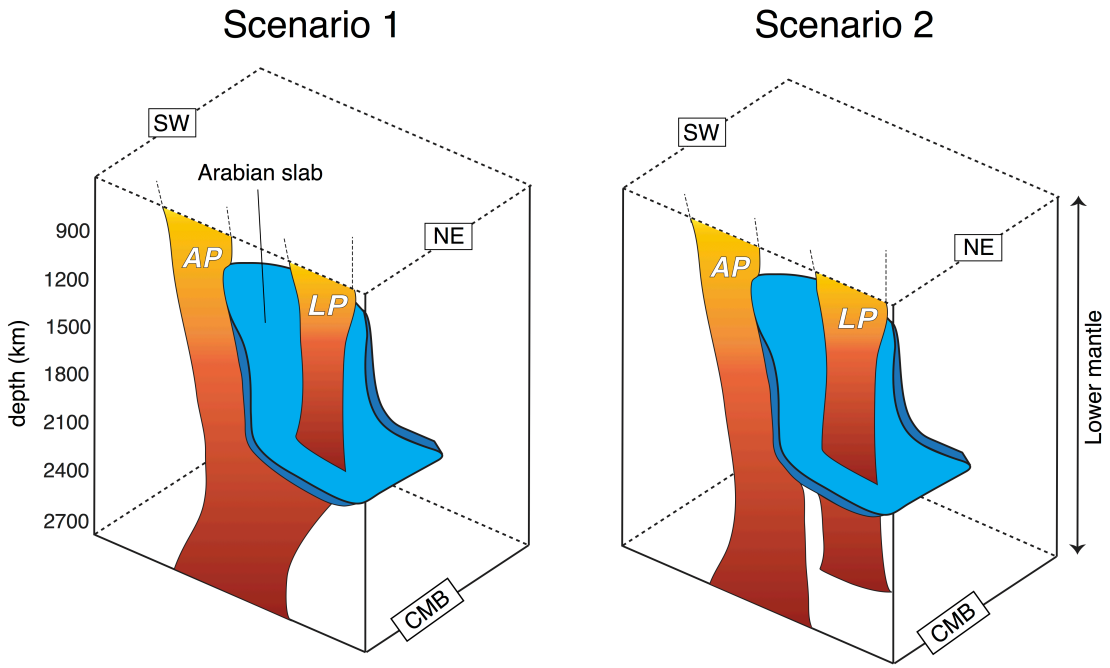

Two proposed scenarios for the source(s) of the Afar and Levant Plumes. Scenario 1 (left panel): the Afar Plume (AP) and Levant Plume (LP) originate at the core-mantle boundary (CMB) from a single source located beneath Arabia and offshore. LP and AP can be splitted in two at mid-mantle depths by the subducted Arabian slab. Scenario 2 (right panel): AP and LP may be originated from two distinct sources in the lowermost mantle and both perturbed by the Arabian slab.

Supplementary Fig. 5.

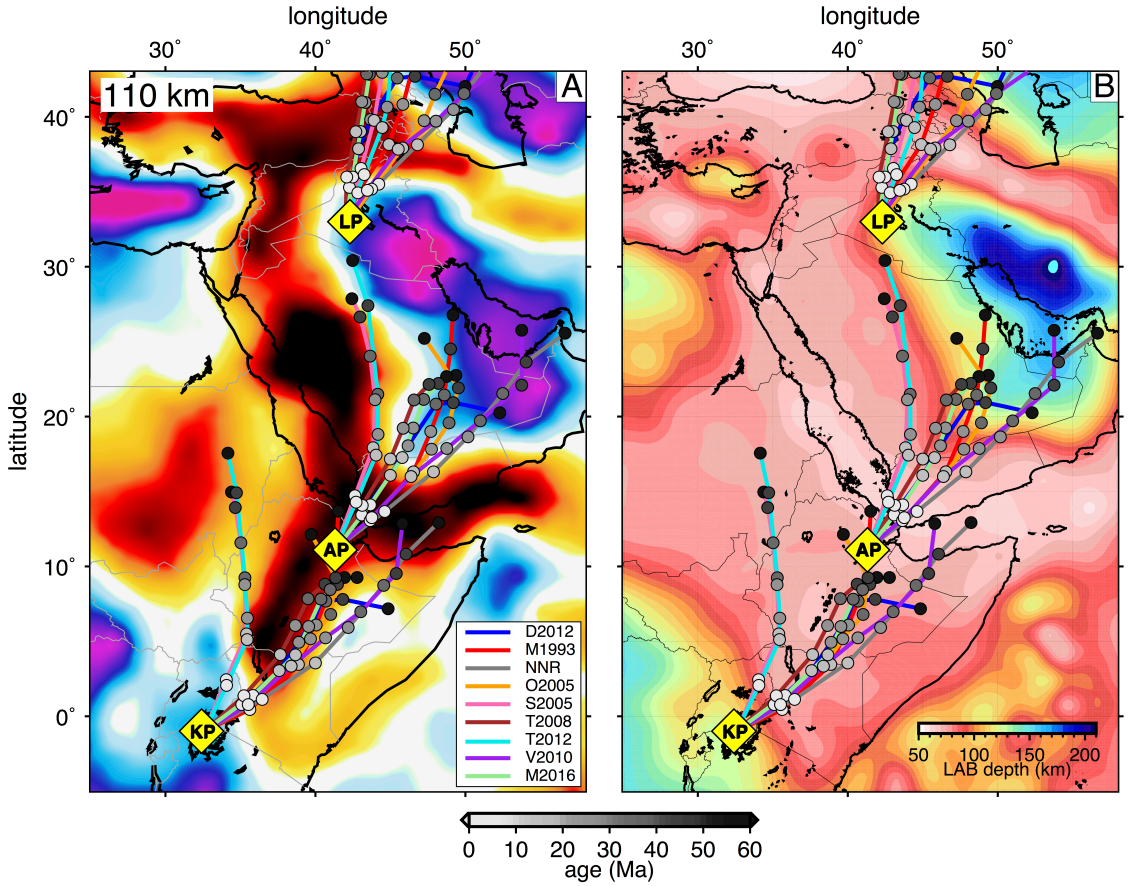

Plume tracks at 0-60 Ma according to different plate-motion models. The models are: D2012 (Doubrovine et al., 2012); M1993 (Muller et al., 1993); NNR (No-Net-Rotation, (Argus et al., 2011); O2005 (O'Neill et al., 2005); S2005 (Schettino & Scotese, 2005); T2008 (Torsvik et al., 2008); T2012 (Torsvik et al., 2012); V2010 (Van Der Meer et al., 2010); M2016 (Matthews et al., 2016). **A.** The map view is the tomographic model plotted at 110 km depth. **B.** The map view is the lithosphere-asthensphere boundary (LAB) depth computed by Fullea et al. (2021). The yellow diamonds indicate the three plumes: KP (Kenya Plume), AP (Afar Plume), and LP (Levant Plume).The different tracks show the variability of results depending on how the plate motion model was built. The dots are coloured according to the age, in Ma.